IET Microwaves, Antennas & Propagation

Research Article

IET Journals
The Institution of Engineering and Technology

Ultra wideband antenna design using discrete Green's functions in conjunction with binary particle swarm optimisation

ISSN 1751-8725
Received on 7th April 2015
Revised on 27th August 2015
Accepted on 1st September 2015
doi: 10.1049/iet-map.2015.0415
www.ietdl.org

Salma Mirhadi ✉, *Nader Komjani*, *Mohammad Soleimani*

Department of Electrical Engineering, Iran University of Science and Technology, Narmak, Tehran, Iran
✉ *E-mail: s_mirhadi@iust.ac.ir*

Abstract: The binary particle swarm optimisation (BPSO) in conjunction with the time-domain discrete Green's function (DGF) method is proposed for designing of printed ultra wideband (UWB) antennas. In the DGF method, on one hand, a three-dimensional problem is reduced to a two-dimensional one, and on the other hand, the broadband frequency characteristics of the antenna are achieved with a single simulation run. Furthermore, the spatial discrete representation of the current on the antenna, in the DGF method, facilitates implementation of its combination with the BPSO algorithm. Two different UWB antennas are designed using the proposed approach. First, an antenna is designed to minimise voltage standing wave ratio (VSWR). The experimental result shows that the antenna has a VSWR about <1.5 over the UWB range. Second, an antenna is designed to have not only low VSWR, but also stable radiation pattern over the UWB range. The experimental results show a good impedance matching and stable omnidirectional pattern over the UWB range.

1 Introduction

The dyadic finite-difference time-domain (FDTD) compatible Green's functions, referred to as the discrete Green's functions (DGFs), were proposed in infinite free space initially [1]. The DGFs were then applied to analysis of antennas with the aim of avoiding the need for absorbing boundary conditions and calculation of free space nodes around them [2–5]. Recently, the DGFs in multilayered media have been derived based on the finite-difference scheme of time-domain mixed-potential equations [6]. The DGFs, which are in the time-domain, are different from the discretised version of continuous Green's functions and reflect the attributes of the discrete solution such as dispersion and stability [7]. The multilayered DGFs have potential applications in printed antenna modelling especially broadband printed antennas. In the DGF method, the current distributions on an antenna have the same discrete scheme as the fields in the Yee grid of the FDTD method and are computed at time successive steps regardless of the white space around the antenna [3, 6].

During the last decades, with the advancement of computer resources, various optimisation techniques have been combined with proper electromagnetic (EM) simulation tools to discover new structures for antennas with superior performance [8–12]. The aim of this paper is to apply DGF method as an EM simulation tool in optimisation process of printed ultra wideband (UWB) antennas. The binary particle swarm optimisation (BPSO) is used to determine the optimal shape of antennas according to a desired performance. Compared with other binary optimisation algorithms, the advantages of BPSO are that BPSO is easy to implement and there are few parameters to adjust [9, 13]. So far, the particle swarm optimisation (PSO) algorithm in combination with different EM simulators, such as method of moment (MoM) or FDTD simulators, has been used to design wideband antennas [13–16]. The combination of the PSO algorithm and the DGF simulator has the advantages of the both FDTD and MoM simulators. In other words, on one hand, since the DGF simulation is in the time-domain such as FDTD method, the broadband frequency characteristics are obtained through a single simulation run [3, 5]. On the other hand, computations are performed only on the antenna regardless of the free space nodes around it, such as MoM simulator [4]. Furthermore, the proposed algorithm is found to be

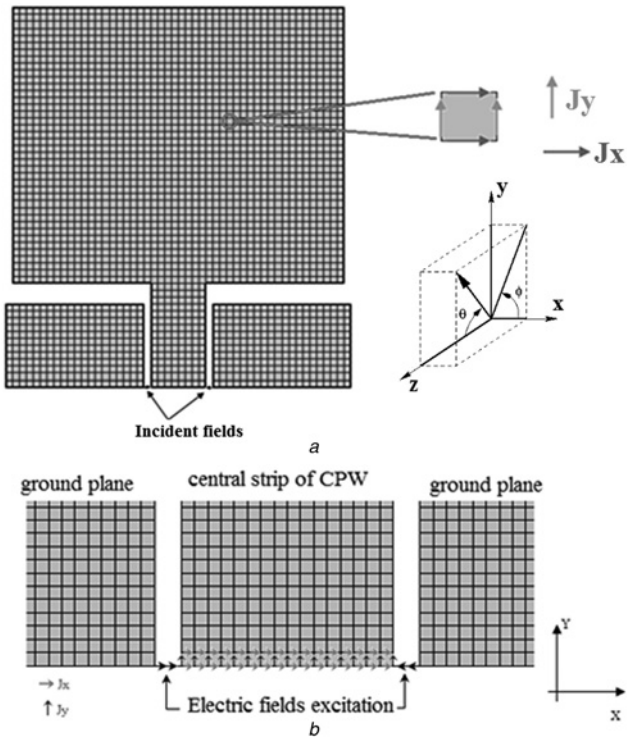

Fig. 1 *Schematic of the mesh on the antenna and the distribution of the discrete currents*

a Schematic of the mesh on the antenna in the DGF method and the distribution of the discrete currents (J_x and J_y) of one cell
b Portion of the mesh grid with representation of the excitation and current distribution at the feed location

© The Institution of Engineering and Technology 2016

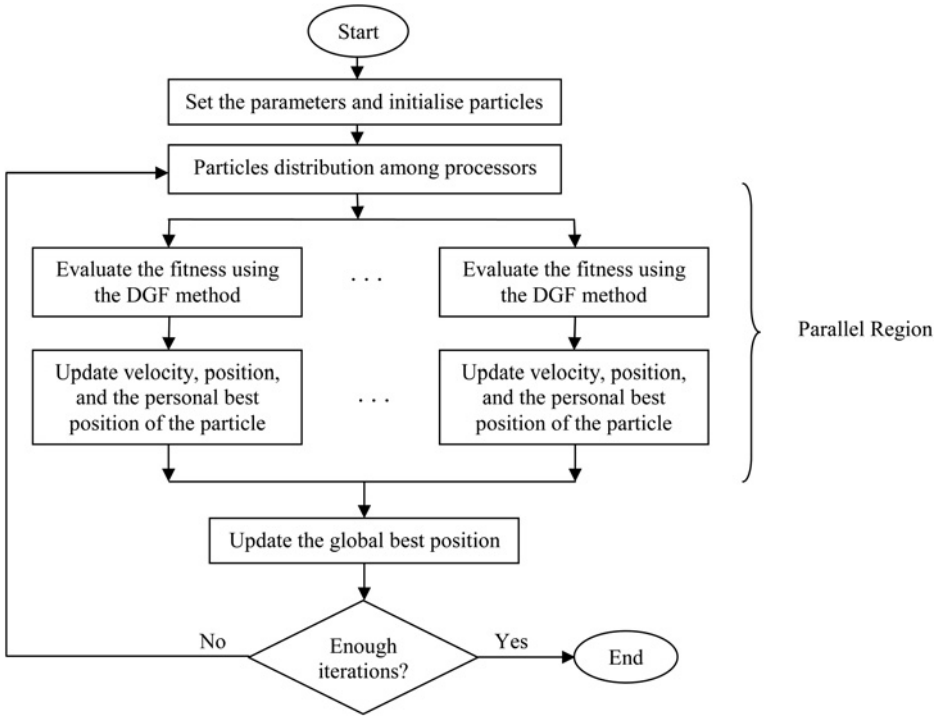

Fig. 2 *Flowchart of the parallel BPSO/DGF algorithm*

highly efficient in terms of programming because of the discrete nature of the DGF method and the BPSO algorithm. This procedure also offers an automatic shape design of UWB antennas to which little attention has been paid [17–19].

In this paper, in addition to the minimum return loss, the stable radiation pattern is considered in the design procedure. Up to now, various techniques have been introduced to enhance pattern stability of the UWB antenna [20–24]. These techniques are based on the previous knowledge of the pre-defined structures. However, in the proposed design the proper geometric shape of a UWB antenna is constructed.

2 Formulation

2.1 Antenna analysis using the DGF method

This paper is focused on shaping of a coplanar waveguide (CPW)-fed planar monopole antenna printed on a dielectric substrate. For the analysis of the antenna using the DGF method, first, the medium is meshed and a space point in a uniform rectangular lattice is demonstrated as $(i, j, k) = (i\Delta x, j\Delta y, k\Delta z)$, where Δx, Δy, and Δz are, respectively, the lattice space increments in the x-, y-, and z-coordinate directions. The DGF of a three-layered medium

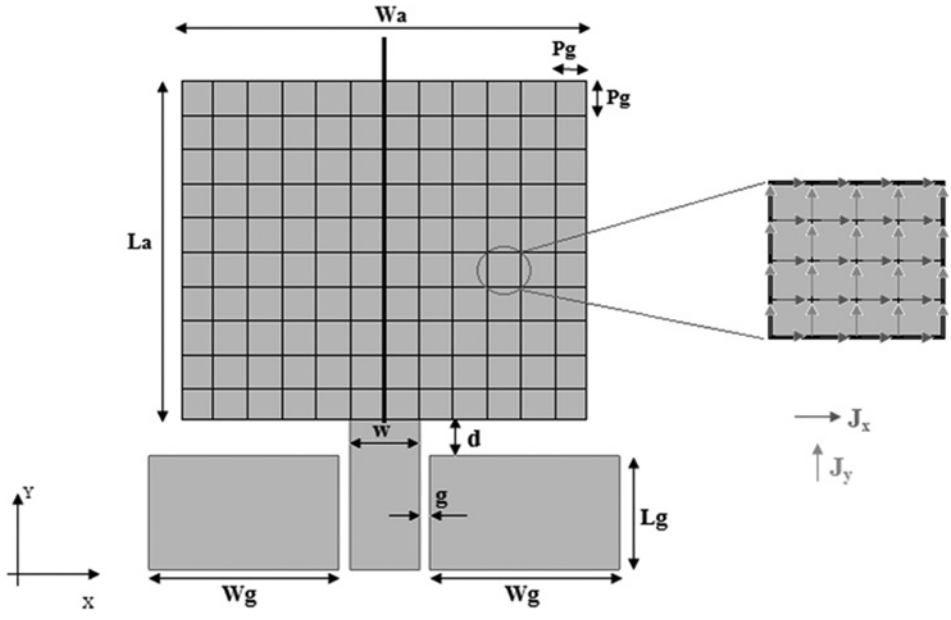

Fig. 3 *Geometry of the monopole antenna with the pixelised patch (L_a = 16 mm and W_a = 19.2 mm) and its fixed ground plane and feed line (w = 3.2 mm, d = 1.2 mm, g = 0.4, W_g = 8 mm, L_g = 4.8 mm). The distribution of the current of a pixel, in the DGF method, is also enlarged*

© The Institution of Engineering and Technology 2016

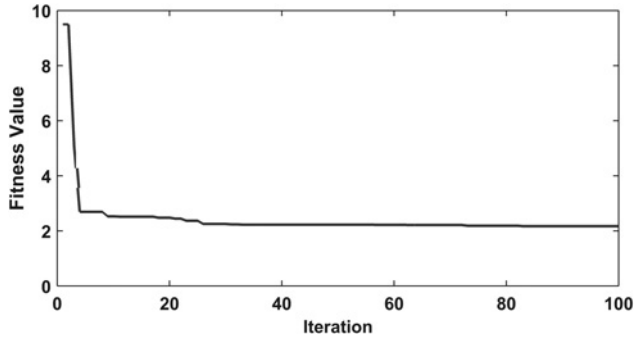

Fig. 4 *Convergence curve of the global best fitness by using 32 particles for 100 iterations in the design of a UWB antenna with minimum return loss*

(air-dielectric-air) are calculated according to [6] and those that are on the surface of the antenna are saved. Then, the induced currents of the antenna at the time step ($n\Delta t$) can be formulated as (1) in terms of the incident field in the future and the currents induced on the structure previously in an iterative fashion [2–3, 6].

$$[\vec{J}]^{n}_{i,j,k} = \frac{\varepsilon_{\text{avg}}}{\Delta t}[\vec{E}_{\text{inc}}]^{n+1/2}_{i,j,k} + \frac{\varepsilon_{\text{avg}}}{\Delta t}\sum_{n'=0}^{n-1}\sum_{i',j',k'}[\bar{G}]^{n-n'}_{i-i',j-j',k-k'}[\vec{J}]^{n'}_{i',j',k'} \quad (1)$$

i, j, k, i', j', k' on the antenna.

where $[\bar{G}]$ is the three-layered discrete Green's functions, $[\vec{J}]$ is the density of the electric current, and ε_{avg} is the effective dielectric constant which is assigned to the cells on the interface and is the average value of the dielectric constants. Fig. 1*a* shows the

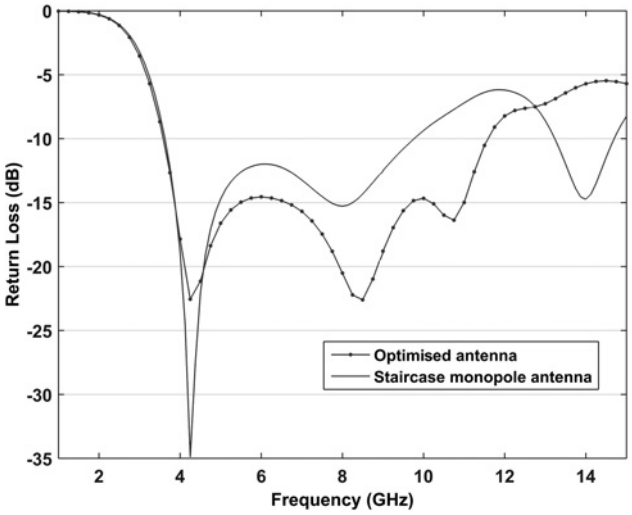

Fig. 6 *Comparison between the return loss of the optimised antenna and the staircase monopole antenna*

schematic of the mesh on the antenna and the distribution of the discrete currents (J_x and J_y) of one cell (the antenna thickness has been considered zero). A portion of the mesh grid showing the excitation and current distribution at the feed location is shown in the Fig. 1*b*. The *x*-directed incident electric fields are between the central strip and the ground planes and are 180° out of phase in the two slots from which the CPW is excited in the even mode.

After launching the excitation, the transient currents are computed at successive time steps by using (1). The voltage and the current at

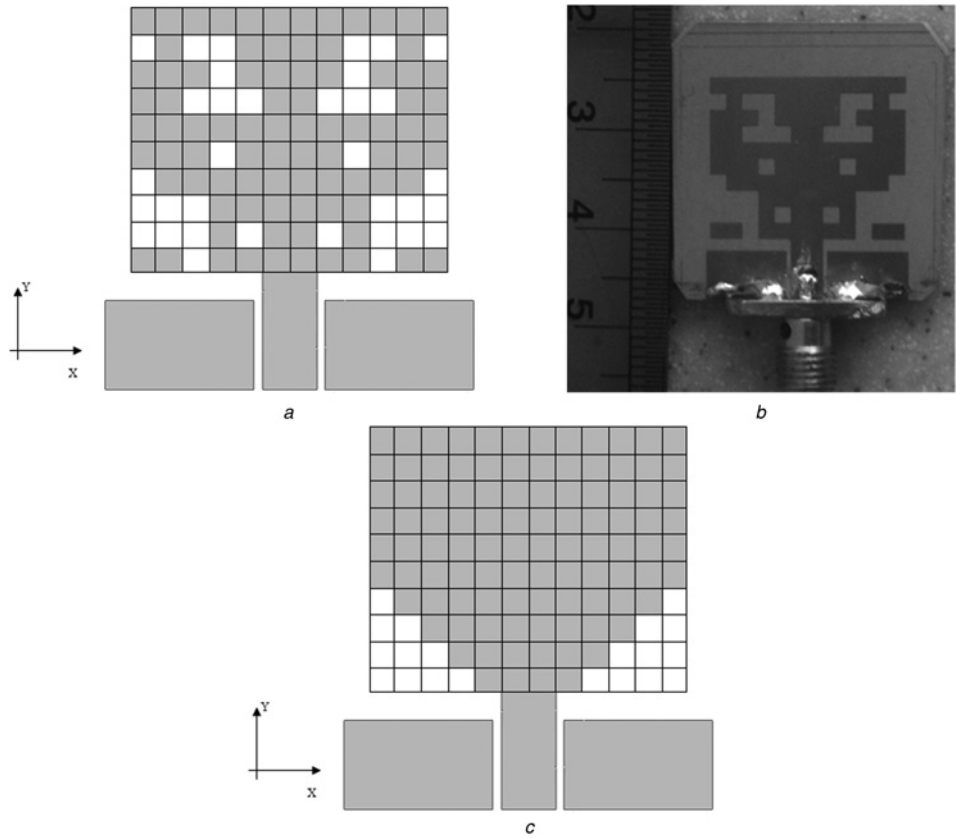

Fig. 5 *Optimum topology of the monopole antenna and its fabricated prototype*

a Optimum topology of the UWB antenna with minimum return loss
b Photograph of the fabricated antenna
c Staircase monopole antenna which is the initial solution and is considered as a reference to compare the results

IET Microw. Antennas Propag., 2016, Vol. 10, Iss. 2, pp. 184–192
© The Institution of Engineering and Technology 2016

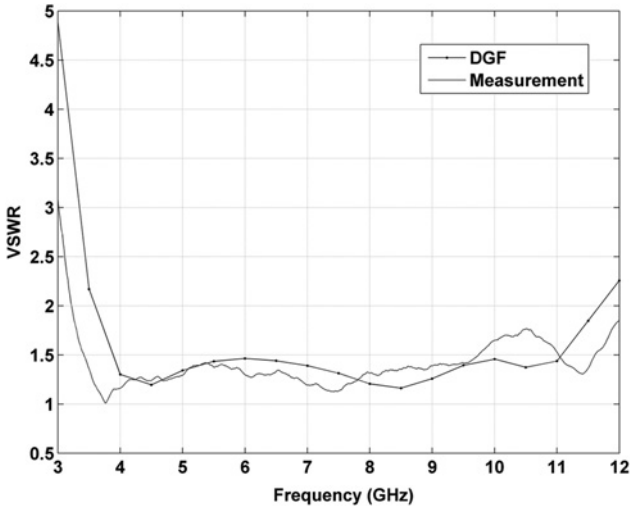

Fig. 7 *Simulated and measured VSWR of the optimised antenna*

the feed location are defined as follows

$$V^n = \Delta x\, n_{\text{xslot}} \frac{(E^{n+1/2}_{\text{xinc}} + E^{n-1/2}_{\text{xinc}})}{2} \tag{2}$$

$$I^n = \Delta x\, \Delta z \sum_i J^n_{y\,i,j=1};\ i \text{ on the centre conductor} \tag{3}$$

where n_{xslot} is the number of nodes in the slot. Then, the input impedance of the antenna can be determined by using the Fourier transform of (2) and (3).

The far-field radiation patterns are obtained by applying fast Fourier transform (FFT) to the time-domain current distribution of (1) and by using the following equations

$$N_\theta(\theta, \varphi, m\Delta f) = \sum_{i,j} \{JF^m_x(i,j)\cos\theta\cos\varphi\, e^{jkr_x} + JF^m_y(i,j)\cos\theta\sin\varphi\, e^{jkr_y}\}\Delta x\Delta y \tag{4}$$

$$N_\varphi(\theta, \varphi, m\Delta f) = \sum_{i,j} \{-JF^m_x(i,j)\sin\varphi\, e^{jkr_x} + JF^m_y(i,j)\cos\varphi\, e^{jkr_y}\}\Delta x\Delta y \tag{5}$$

where

$$r_x = (i+0.5)\Delta x\sin\theta\cos\varphi + (j)\Delta y\sin\theta\sin\varphi$$
$$r_y = (i)\Delta x\sin\theta\cos\varphi + (j+0.5)\Delta y\sin\theta\sin\varphi$$

$JF^m_{x,y}$ is FFT of the current with frequency steps of $m\Delta f$ where $\Delta f = 1/(\Delta t N_t)$ and N_t is the total number of time steps in DGF simulation.

2.2 Binary PSO algorithm

PSO, developed in 1995 by Kennedy and Eberhart [25], is a robust stochastic optimisation technique inspired by the movement of animal swarms. It uses a number of agents (particles) moving in the search space to look for the best solution. Each particle adjusts its flying according to its personal best flying experience as well as the swarm's best flying experience. A discrete binary version of PSO was also proposed by Kennedy and Eberhart [26] in which each particle has to take a binary decision. The details of PSO and BPSO theory are introduced well and will not be repeated here.

2.3 BPSO/DGF algorithm

In optimising process the design space is divided into N pixels and the optimal design has to be explored in a solution domain. Each candidate design (particle) is represented by a binary string consisting of a series of '0's and '1's. The antenna topology of the

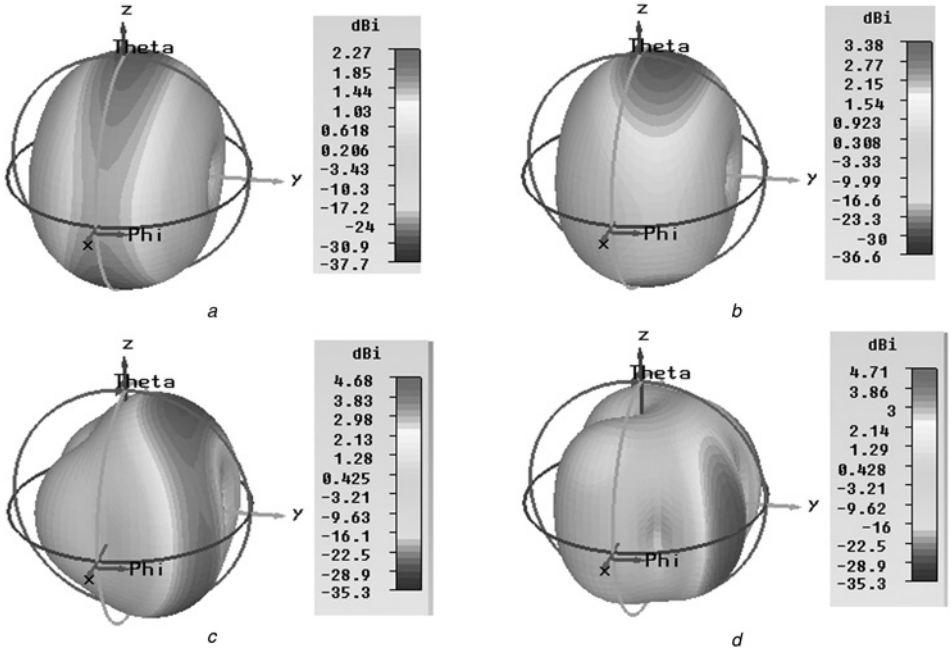

Fig. 8 *Simulated 3D radiation patterns of the first antenna at*

a 3.5 GHz
b 6 GHz
c 9 GHz
d 10.5 GHz

© The Institution of Engineering and Technology 2016

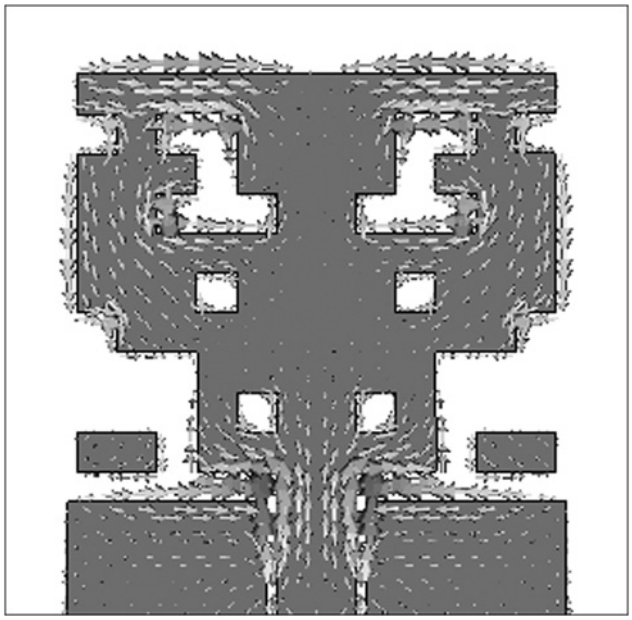

Fig. 9 *Current distribution of the antenna at 10.5 GHz*

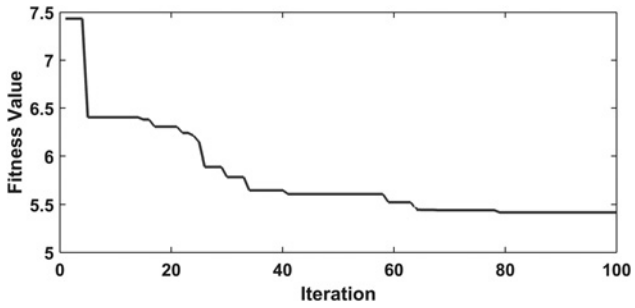

Fig. 10 *Convergence curve of the global best fitness by using 32 particles for 100 iterations in the design of a UWB antenna with minimum return loss and stable radiation pattern*

each particle is constructed in accordance with the binary string such that the absence and presence of the metal correspond to '0's and '1's from the binary string, respectively. The fitness function of each particle is evaluated by the DGF method. Since the DGF simulations for each particle within an iteration are independently implemented, the optimisation process is performed on parallel clusters. The parallel implementation allows less computational time and better optimisation efficiency. The BPSO/DGF code has been written in FORTRAN in which parallelisation can be implemented using the OpenMP application program interfaces (API) [27]. Fig. 2 shows the flowchart of the parallel BPSO/DGF algorithm. The OpenMP FORTRAN API follows the fork-join model of parallel execution. In this model, the program starts with a single thread called master thread to set the parameters of the program and initialise the particles. Whenever an OpenMP parallel construct is encountered, a team of threads (slave threads) is created. They simultaneously execute the DGF method to evaluate performance of each candidate design (particle). According to the DGF results, velocity, position, and personal best of each particle are updated. At the end of the parallel construct, team threads synchronise and the master thread collects the results to determine the global best position of the solution space.

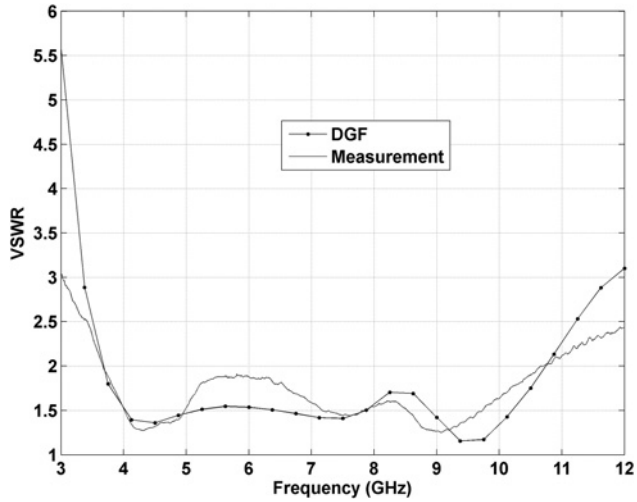

Fig. 12 *Simulated and measured VSWR of the optimised antenna*

3 Antenna design

Fig. 3 shows a CPW-fed planar monopole antenna printed on a Rogers RT6002 substrate with thickness of 1.6 mm and relative permittivity of 2.94. Its rectangular monopole patch with sides of 16 mm × 19.2 mm is defined as the design domain and is discretised into square pixels with a side length of P_g. The geometric dimensions of the ground plane and feed line are supposed to be fixed and shown in Fig. 3. In the DGF analysis, the spatial and time increments are set to $\Delta x = \Delta y = \Delta z = 0.4$ mm and $c\Delta t = 0.5\Delta x$, respectively. The parameter P_g is chosen such that the $P_g/\Delta x$ (or $P_g/\Delta y$) is an integer greater than one. With $P_g =$ 1.6 mm, $P_g/\Delta x$ (or $P_g/\Delta y$) is equal to 4 and 4 × 4 DGF cells completely cover each pixel as shown in the enlarged view of a

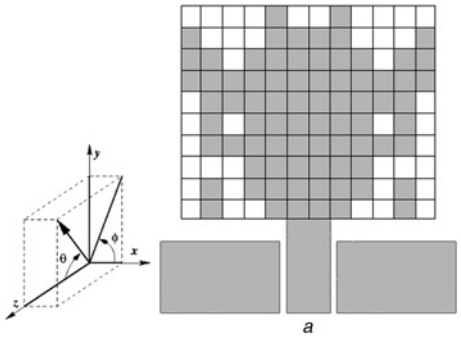

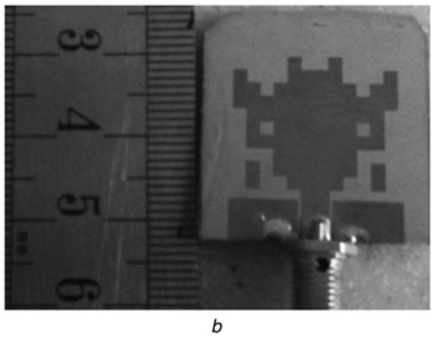

Fig. 11 *Optimum topology of the antenna and its fabricated prototype*

a Optimum topology of the UWB antenna with low VSWR and stable radiation pattern
b photograph of the fabricated antenna

IET Microw. Antennas Propag., 2016, Vol. 10, Iss. 2, pp. 184–192
© The Institution of Engineering and Technology 2016

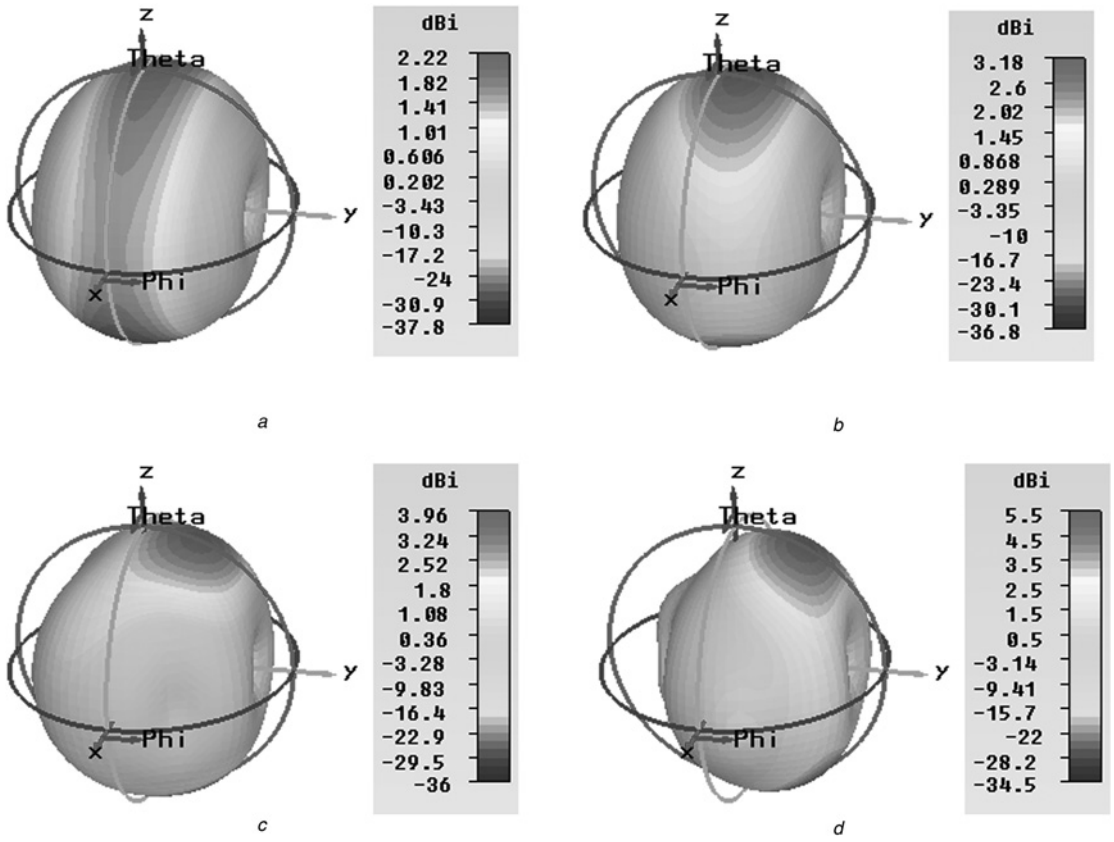

Fig. 13 *Simulated 3D radiation patterns of the second antenna at*

a 3.5 GHz
b 6 GHz
c 9 GHz
d 10.5 GHz

pixel in Fig. 3. With these choices and by considering the symmetric shape of the antenna with respect to the *y*–*z* plane, the number of the pixels or the length of the binary strings is 60. The geometry refinement technique is also applied during optimisation to avoid the point contact of the conductors resulting in an easy fabrication [28].

3.1 UWB antenna design with minimum voltage standing wave ratio (VSWR)

In this design, the fitness function is defined as

$$F = \max(\mathrm{VSWR}(f))\big|_{f\in[3.1\,\mathrm{GHz},\ 10.6\,\mathrm{GHz}]} \tag{6}$$

to minimise VSWR of the antenna over the UWB band.

As observed from [10], in the 100-D binary optimisation problem, a swarm with a number of 50 agents was adequate to obtain a reasonably good convergence. In fact, in BPSO, the need for a large number of agents is not as demanding as in Real PSO probably due to the binary polarity of each dimension instead of the infinite set in continuous spaces [29]. Our problem is 60-dimensional and we have selected 32 particles. In addition, the optimisation process utilises eight parallel processors for parallel implementation. Therefore, for a 32-particle swarm, DGF simulation is repeated four times within each iteration of optimisation to evaluate objective function of all particles. The optimisation was stopped after 100 iterations. Fig. 4 plots the convergence curve of the global best fitness value for 100 iterations which indicates a good convergence during 100 iterations.

Fig. 5*a* and *b* illustrates the optimum topology of the monopole antenna and its fabricated prototype, respectively. Furthermore, the initial solution which has been selected as a staircase monopole antenna is shown in Fig. 5*c*. It is similar to a beveled square monopole antenna known as a wideband antenna [30].

The return loss of the optimised monopole antenna and the staircase monopole antenna are compared in Fig. 6. The simulated and measured results of the VSWR for the optimised antenna are

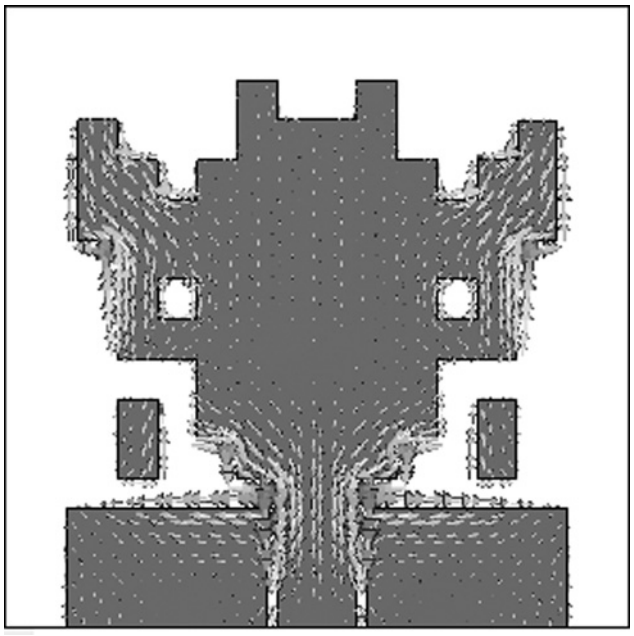

Fig. 14 *Current distribution of the second antenna at 10.5 GHz*

© The Institution of Engineering and Technology 2016

shown in Fig. 7. It can be seen that the optimised antenna has very good impedance matching over the UWB band.

The simulated 3D radiation patterns of the antenna at different frequencies are shown in Fig. 8. At 3.5 and 6 GHz, the radiation patterns look such as a donut, similar to a monopole antenna. At the 9 GHz, the pattern changes its shape to a pinched donut and the maximum radiation tilts from the broadside direction. It can be seen that, at 10.5 GHz, the antenna's radiated fields become destructive in the broadside direction and a null appears. In fact, at the higher frequencies, the EM wave of the antenna operates in a travelling wave mode and needs to travel down to the antenna structure. If the travelling length of the current is big in terms of the wavelength, a null appears in the broadside direction [20]. The length of the current path is half the perimeter of the antenna

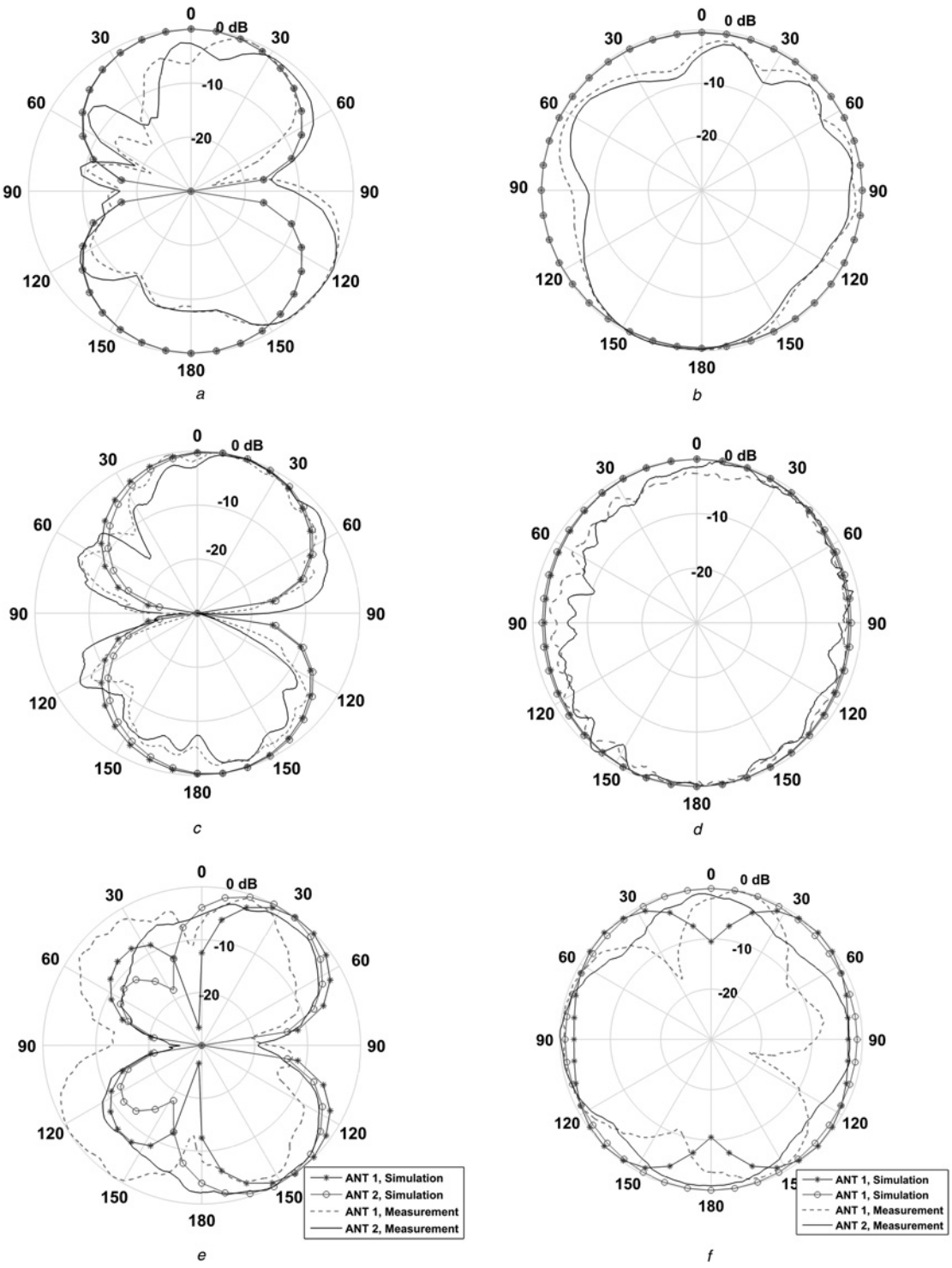

Fig. 15 *Measured and simulated radiation patterns of the first and second antenna at 3.5 GHz*

a In the *E*-plane
b In the *H*-plane, at 6 GHz
c In the *E*-plane
d In the *H*-plane, and at 10.5 GHz
e In the *E*-plane
f In the *H*-plane

IET Microw. Antennas Propag., 2016, Vol. 10, Iss. 2, pp. 184–192
© The Institution of Engineering and Technology 2016

which is shown in Fig. 9. It is about 36.8 mm and greater than of the wavelength at 10.6 GHz (28 mm). This problem is also seen in the radiation pattern of the staircase monopole antenna at 10.5 GHz.

3.2 UWB antenna design with low VSWR and stable radiation pattern

Because of the radiation pattern degradation of the previously designed antenna at the higher frequencies, in this section, we have designed an UWB antenna with low VSWR and stable radiation pattern. The desired radiation pattern is monopole-like radiation pattern producing a figure of eight radiation pattern in the *E*-plane (*y*–*z* plane) and omnidirectional radiation pattern in the *H*-plane (*x*–*z* plane). Therefore, the objective function is defined as

$$F = F_1 + F_2 + F_3 \tag{7}$$

$$F_1 = \max(\mathrm{VSWR}(f))\big|_{f\in\,[3.1\,\mathrm{GHz},\ 10.6\,\mathrm{GHz}]} \tag{8}$$

$$F_2 = \frac{1}{N_f}\sum_{f_j} \max_\theta(|E(\theta,\ \varphi = 0,\ f_j) - E(\theta_{\max},\ \varphi = 0,\ f_j)|) \tag{9}$$

$$F_3 = \frac{1}{N_f}\sum_{f_j} (|E(\theta = 0,\ \varphi = 90,\ f_j) - E(\theta_{\max},\ \varphi = 90,\ f_j)|) \tag{10}$$

where $E(\theta, \varphi, f_j)$ is the normalised radiated electric field at frequency f_j in the angular direction of (θ, φ) according to the coordinate system shown in Fig. 11*a*. The sampled frequencies $f_j (j = 1, \ldots, N_f;\ N_f = 4)$ for pattern optimisation are {3.5, 6, 9, 10.5} GHz. The objective function F_2 minimises the maximum deviation of the radiation pattern from its maximum value at frequency f_j and in the *H*-plane to attain an omnidirectional pattern which has equal amplitude in all the directions. The objective function F_3 minimises the deviation of the radiation pattern in the broadside direction ($\theta = 0$) from its maximum value at frequency f_j and in the *E*-plane to achieve maximum radiation at broadside. The number of particles and iterations are the same as previous section. The convergence curve of the global best fitness value for 100 iterations is illustrated in Fig. 10. It has a good convergence during 100 iterations. The optimum topology of the antenna and its fabricated prototype are shown in Fig. 11. The simulated and measured results of the VSWR are shown in Fig. 12. The measured VSWR of the antenna is <2 in the frequency range 3.72–10.58 GHz.

The simulated 3D radiation patterns of the second antenna at different frequencies are shown in Fig. 13. Stable boresight radiation patterns are clearly observed at different frequencies in this design in comparison with those of Fig. 8. The current distribution on the antenna at 10.5 GHz is shown in Fig. 14. The effective length of the current path is about 22.4 mm which is shorter than the wavelength; therefore, no null appears in the broadside direction.

The simulated and measured normalised radiation patterns of the first and second antennas in the *H*- and *E*-planes at different frequencies are shown in Fig. 15. At lower frequencies, the ripples occur in the measured radiation patterns which are mainly caused by the feeding cable used to connect the antennas with the small ground plane to the measurement system. This effect can be alleviated by using the cable enclosed by an EM interference suppressant tube to absorb EM radiation [31]. In spite of this, the radiation patterns of both designed antennas are similar at lower frequencies. However, it is seen that the second antenna provides more stable omnidirectional radiation pattern than that of the first antenna at 10.5 GHz in the *H*-plane (Fig. 15*f*). It is also clear that, at 10.5 GHz, a null appears in the broadside radiation pattern of the first antenna in the *E*-plane which leads a drop of more than 6 dB in the radiated power of the first antenna compared with the second antenna (Fig. 15*e*).

4 Conclusions

In this paper, integration of the BPSO algorithm and the DGF method is presented in the design of the printed UWB antennas. The discrete nature of both methods greatly simplifies the implementation. The design procedure is a topology optimisation which does not require any details of the antenna template. The optimisation is carried out for two different designs. In the first one, proper topology of the antenna for the minimum VSWR is achieved. In the second one, an appropriate topology is explored not only for the low VSWR but also for the stable radiation pattern in the entire UWB range. The experimental results confirm the validity of the design algorithm.

5 References

1 Vazquez, J., Parini, C.G.: 'Discrete Green's function formulation of FDTD method for electromagnetic modelling', *Electron. Lett.*, 1999, **35**, (7), pp. 554–555
2 Vazquez, J., Parini, C.G.: 'Antenna modelling using discrete Green's function formulation of FDTD method', *Electron. Lett.*, 1999, **35**, (13), pp. 1033–1034
3 Ma, W., Rayner, M.R., Parini, C.G.: 'Discrete Green's function formulation of the FDTD method and its application in antenna modeling', *IEEE Trans. Antennas Propag.*, 2005, **53**, (1), pp. 339–364
4 Mirhadi, S., Soleimani, M., Abdolali, A.: 'Discrete Green's function approach for the analysis of a dual band-notched UWB antenna', *Microw. Opt. Tech. Lett*, 2013, **55**, (9), pp. 2168–2174
5 Mirhadi, S., Soleimani, M., Abdolali, A.: 'UWB antennas analysis using FDTD-based discrete Green's function approach', *IEEE Antennas Wirel. Propag. Lett.*, 2013, **12**, pp. 1089–1093
6 Mirhadi, S., Soleimani, M., Abdolali, A.: 'Multilayered discrete Green's functions based on mixed-potential finite-difference formulation', *IEEE Trans. Antennas Propag..*, 2014, **62**, pp. 5765–5774
7 Kastner, R.: 'A multidimensional Z-transform evaluation of the discrete finite difference time domain Green's function', *IEEE Trans. Antennas Propag.*, 2006, **54**, (4), pp. 1215–1222
8 Rocca, P., Oliveri, G., Massa, A.: 'Differential evolution as applied to electromagnetics', *IEEE Antennas Propag. Mag.*, 2011, **53**, (1), pp. 38–49
9 Rocca, P., Benedetti, M., Donelli, M., *et al.*: 'Evolutionary optimization as applied to inverse problems', *Inverse Probl.*, 2009, **25**, pp. 1–41
10 Jin, N., Rahmat-Samii, Y.: 'Advances in particle swarm optimization for antenna designs: real-number, binary, single-objective and multiobjective implementations', *IEEE Trans. Antennas Propag.*, 2007, **55**, (3), pp. 556–567
11 Khodier, M., Al-Aqil, M.: 'Design and optimisation of Yagi-Uda antenna arrays', *IET Microw. Antennas Propag.*, 2008, **4**, (4), pp. 426–436
12 Chamaani, S., Mirtaheri, S.A., Paran, *et al.*: 'Coplanar waveguide-fed ultra wideband planar monopole antenna optimisation', *IET Microw. Antennas Propag.*, 2010, **4**, (9), pp. 1264–1274
13 Jin, N., Rahmat-Samii, Y.: 'Parallel particle swarm optimization and finite difference time-domain (PSO/FDTD) algorithm for multiband and wide-band patch antenna designs', *IEEE Trans. Antennas Propag.*, 2005, **53**, (11), pp. 3459–3468
14 Lizzi, L., Viani, F., Azaro, R.: 'A PSO-driven spline-based shaping approach ultrawideband (UWB) antenna synthesis', *IEEE Trans. Antennas Propag.*, 2008, **56**, (8), pp. 2613–2620
15 Dadgarour, A., Dadashzadeh, G., Naser-Moghadasi, M., *et al.*: 'Design and optimization of compact balanced antipodal staircase bow-tie antenna', *IEEE Antennas Wirel. Propag. Lett.*, 2013, **12**, pp. 1089–1093
16 Martin, J.E., Pantoja, M.F., Bretones, A.R., *et al.*: 'Exploration of multi-objecive particle swarm optimizaion on the design of UWB antennas'. Third European Conf. on Antennas and Propagation, Berlin, Germany, March 2009, pp. 561–565
17 John, M., Ammann, M.J.: 'Wideband printed monopole design using a genetic algorithm', *IEEE Antennas Wirel. Propag. Lett.*, 2007, **6**, pp. 447–449
18 Ding, M., Jin, R., Geng, J., *et al.*: 'Auto-design of band-notched UWB antennas using mixed model of 2D GA and FDTD', *Electron. Lett.*, 2008, **44**, (4), pp. 257–258
19 Hassan, E., Wadbro, E., Berggren, M.: 'Topology optimization of metallic antennas', *IEEE Trans. Antennas Propag.*, 2014, **62**, (5), pp. 2488–2500
20 Fereidoony, F., Chamaani, S., Mirtaheri, S.A.: 'Systematic design of UWB monopole antennas with stable omnidirectional radiation pattern', *IEEE Antennas Wirel. Propag. Lett.*, 2012, **11**, pp. 752–755
21 Wu, Q., Jin, R., Geng, J., *et al.*: 'Printed omni-directional UWB monopole antenna with very compact size', *IEEE Trans. Antennas Propag.*, 2008, **56**, (3), pp. 896–899
22 Yang, X.S., Tat Ng, K., Yeung, S.H., *et al.*: 'Jumping genes multiobjective optimization scheme for planar monopole ultrawideband antenna', *IEEE Trans. Antennas Propag.*, 2008, **56**, (12), pp. 3659–3666
23 Valderas, D., de No, J., Melendez, J., *et al.*: 'Design of omnidirectional broadband metal-plate monopole antennas', *Microw. Opt. Tech. Lett*, 2007, **49**, (2), pp. 375–379
24 Wong, K.L., Su, S.W., Tang, C.L.: 'Broadband omnidirectional metal-plate monopole antenna', *IEEE Trans. Antennas Propag.*, 2005, **53**, (1), pp. 581–583

© The Institution of Engineering and Technology 2016

25 Kennedy, J., Eberhart, R.: 'Particle swarm optimization', *Proc. IEEE Int. Conf. Neural Network*, 1995, **4**, pp. 1942–1948
26 Kennedy, J., Eberhart, R.: 'A discrete binary version of the particle swarm algorithm', *Proc. IEEE Int. Conf. Syst. Man Cybern.*, 1997, **5**, pp. 4104–4108
27 OpenMP API, available at http://www.openmp.org
28 Ohira, M., Deguchi, H., Tsuji, M., *et al.*: 'Multiband single-layer frequency selective surface designed by combination of genetic algorithm and geometry-refinement technique', *IEEE Trans. Antennas Propag.*, 2004, **52**, (11), pp. 2925–2931
29 Jin, N.: 'Particle swarm optimization in engineering electromagnetics', (ProQuest, United States of America, 2008), pp. 54–55
30 Ammann, M.J.: 'Control of the impedance bandwidth of wideband planar monopole antennas using a beveling technique', *Microw. Opt. Tech. Lett*, 2001, **30**, (4), pp. 229–232
31 Abdul Matin, M.: 'Cable effects on measuring small planar UWB monopole antennas', in 'Ultra wide band-current status and future trends' (InTech, Croatia, 2012), DOI: 10.5772/2588

© The Institution of Engineering and Technology 2016

Copyright of IET Microwaves, Antennas & Propagation is the property of Institution of Engineering & Technology and its content may not be copied or emailed to multiple sites or posted to a listserv without the copyright holder's express written permission. However, users may print, download, or email articles for individual use.